Monthly Notices of the ROYAL ASTRONOMICAL SOCIETY

MNRAS **514,** 780–789 (2022) https://doi.org/10.1093/mnras/stac1317
Advance Access publication 2022 May 12

Observational properties of puffy discs: radiative GRMHD spectra of mildly sub-Eddington accretion

Maciek Wielgus [1,2,3★] Debora Lančová [4,5★] Odele Straub [6,7] Włodek Kluźniak [5] Ramesh Narayan [2,3] David Abarca,[5] Agata Różańska,[5] Frederic Vincent,[8] Gabriel Török [4] and Marek Abramowicz[4,5,9]

[1]*Max-Planck-Institut für Radioastronomie, Auf dem Hügel 69, D-53121 Bonn, Germany*
[2]*Black Hole Initiative at Harvard University, 20 Garden Street, Cambridge, MA 02138, USA*
[3]*Center for Astrophysics | Harvard & Smithsonian, 60 Garden Street, Cambridge, MA 02138, USA*
[4]*Research Center for Computational Physics and Data Processing, Institute of Physics, Silesian University in Opava, 746-01 Opava, Czech Republic*
[5]*Nicolaus Copernicus Astronomical Centre, Polish Academy of Sciences, Bartycka 18, PL-00-716 Warsaw, Poland*
[6]*ORIGINS Excellence Cluster, Boltzmannstraße 2, D-85748 Garching, Germany*
[7]*Max Planck Institute for Extraterrestrial Physics, Gießenbachstraße 1, D-85748 Garching, Germany*
[8]*LESIA, Observatoire de Paris, Université PSL, CNRS, Sorbonne Universités, UPMC Université Paris 06, Université de Paris, Sorbonne Paris Cité, 5 place Jules Janssen, F-92195 Meudon, France*
[9]*Department of Physics, Göteborg University, SE-412-96 Göteborg, Sweden*

Accepted 2022 May 5. Received 2022 May 5; in original form 2022 February 17

ABSTRACT

Numerical general relativistic radiative magnetohydrodynamic simulations of accretion discs around a stellar-mass black hole with a luminosity above 0.5 of the Eddington value reveal their stratified, elevated vertical structure. We refer to these thermally stable numerical solutions as puffy discs. Above a dense and geometrically thin core of dimensionless thickness $h/r \sim 0.1$, crudely resembling a classic thin accretion disc, a puffed-up, geometrically thick layer of lower density is formed. This puffy layer corresponds to $h/r \sim 1.0$, with a very limited dependence of the dimensionless thickness on the mass accretion rate. We discuss the observational properties of puffy discs, particularly the geometrical obscuration of the inner disc by the elevated puffy region at higher observing inclinations, and collimation of the radiation along the accretion disc spin axis, which may explain the apparent super-Eddington luminosity of some X-ray objects. We also present synthetic spectra of puffy discs, and show that they are qualitatively similar to those of a Comptonized thin disc. We demonstrate that the existing XSPEC spectral fitting models provide good fits to synthetic observations of puffy discs, but cannot correctly recover the input black hole spin. The puffy region remains optically thick to scattering; in its spectral properties, the puffy disc roughly resembles that of a warm corona sandwiching the disc core. We suggest that puffy discs may correspond to X-ray binary systems of luminosities above 0.3 of the Eddington luminosity in the intermediate spectral states.

Key words: accretion, accretion discs – black hole physics – radiative transfer – scattering – software: simulations – X-rays: binaries.

1 INTRODUCTION

Our understanding of accretion on to stellar-mass black holes in X-ray binary systems has been built by five decades of observations following the *Uhuru* satellite mission (Giacconi et al. 1971) and theoretical developments starting with the α-disc solution of Shakura & Sunyaev (1973). The former are reviewed in e.g. Levine et al. (1996) and Remillard & McClintock (2006) and the latter in e.g. Done, Gierliński & Kubota (2007) and Abramowicz & Fragile (2013).

Most known black hole X-ray binaries (BHXBs) undergo a cycle of outbursts, driven by a mass accretion rate modulation caused by an outer disc instability (Homan et al. 2001; Lasota 2001; Bagińska et al. 2021). During outburst, in a luminous ($0.05 < L/L_{\rm Edd} < 0.3$) soft (thermal) spectral state, the observations are consistent with multiblackbody spectra expected from the classic analytical thin α-disc model in its relativistic version (NT disc; Novikov & Thorne 1973; Page & Thorne 1974). However, in the radiation pressure-dominated regime $p_{\rm rad} \gg p_{\rm gas}$, expected in the inner part of the accretion disc, the analytical model is viscously (Lightman & Eardley 1974) and thermally (Shakura & Sunyaev 1976) unstable. Since the observations indicate stability of BHXB accretion discs on relevant time-scales, one must conclude that while the thin disc model is effective in predicting spectra consistent with observations in the applicable luminosity regime (Li et al. 2005; McClintock, Narayan & Steiner 2014), it *is not* a self-consistent and correct description of the physical reality. For larger mass accretion rates, stability

* E-mail: maciek.wielgus@gmail.com (MW); debora.lancova@fpf.slu.cz (DL)

can be achieved through dynamical advection, which removes the excess thermal energy, as found for the (vertically integrated) slim disc models (Abramowicz et al. 1988; Sądowski 2009), but the puzzle remains for the observationally interesting case of mildly sub-Eddington luminosities. Several stabilizing mechanisms have been suggested (e.g. Różańska et al. 1999; Oda et al. 2009; Ciesielski et al. 2012; Zhu & Narayan 2013), and magnetic fields seem to be particularly promising.

At luminosities above $\sim 0.3\, L_{\rm Edd}$, the observed spectra of BHXBs are no longer consistently represented by the thin disc models (McClintock et al. 2006), as the disc geometry begins to deviate from the geometrical thinness assumption. Attempts to utilize the more general theoretical framework of the slim disc model do not fully address the inconsistency (Straub et al. 2011). Unlike thin (or slim) discs, high mass accretion rate flows may in reality include the presence of a warm corona (Zhang et al. 2000; Gronkiewicz & Różańska 2020), increasing the system energetic output in soft X-ray, and/or outflows (Ohsuga et al. 2009), modifying the dynamical structure of the system. The impact of the upper disc layers (disc atmosphere) is typically solved for in separation from the radial disc structure (Davis & Hubeny 2006; Różańska et al. 2011; Sądowski et al. 2011). In numerical simulations, the three-dimensional structure of the accretion disc can be captured self-consistently.[1]

A numerical model of a magnetically stabilized, radiation pressure-dominated, high-luminosity accretion disc in the general relativistic radiative magnetohydrodynamic (GRRMHD) framework has been presented by Sądowski (2016). We have further developed this model in the sub-Eddington case (Lančová et al. 2019), discussing the morphology of the obtained solutions: a dense, geometrically thin disc core is sandwiched by an elevated region of gas with density lower by about two orders of magnitude that nevertheless remains optically thick to scattering. Because of this puffed-up region, supported radially by Keplerian rotation and vertically predominantly by the magnetic pressure, we refer to these solutions as *puffy discs*.

GRRMHD simulations promise an approach in which the relevant physics (magnetic fields, outflows, cooling, turbulence, etc.) is self-consistently taken into account, at the cost of large computational complexity (e.g. Ohsuga & Mineshige 2011; Sądowski et al. 2013, 2014, 2017). In this paper, we discuss the observational properties of puffy discs at luminosity of 0.6–$1.5 L_{\rm Edd}$, inferred from GRRMHD simulations presented in Sądowski (2016) and Lančová et al. (2019). We discuss how these numerical models could yield a theoretical framework for the interpretation of the BHXB spectra beyond the $\sim 0.3 L_{\rm Edd}$ thin disc limit.

2 PUFFY DISCS

2.1 Numerical set-up and conventions

We perform GRRMHD simulations of accretion on to a $10\,{\rm M}_\odot$ Schwarzschild (non-spinning) black hole using KORAL,[2] a highly parallelized GRRMHD code (Sądowski et al. 2013, 2014, 2017). The details of the numerical set-up have been described in Sądowski (2016). The radiative part of the simulation set-up accounts for the electron scattering that dominates the total opacity in the considered regime, as well as free–free absorption and thermal Comptonization (following Sądowski & Narayan 2015). At this stage, frequency-averaged (bolometric) opacities are used, with the aim of capturing the radiation feedback on the disc structure and dynamics. We then use the relativistic radiative post-processing code HEROIC (Zhu et al. 2015; Narayan et al. 2016) to compute puffy disc spectra and images, solving the complete radiative transfer problem on the converged, time-averaged output of GRRMHD models (gas density, temperature, velocity, and magnetic field maps in the inner part of the simulation volume). The simulations were averaged azimuthally over the whole domain, and in time for a period of at least $5000GM/c^3$, corresponding to a converged, quasi-stationary part of the simulation, mostly unaffected by the initial conditions. The contributions from the outer unconverged region of the simulation were masked with an extrapolation procedure (Narayan, Sądowski & Soria 2017) employed for spherical radii $r > 25GM/c^2$. HEROIC solves for the radiation field in both optically thick and optically thin regimes, including the scattering effects.

We consider three post-processed GRRMHD simulation runs, parametrizing the mass accretion rate through the black hole event horizon in Eddington units[3] with $\dot{m} = 0.6$, 0.9, and 1.5 (Sądowski 2016; Lančová et al. 2019). We take

$$\dot{m} \equiv \frac{\dot{M}}{\dot{M}_{\rm Edd}} = \frac{0.057 \dot{M} c^2}{L_{\rm Edd}}\,, \tag{1}$$

where we defined the Eddington mass accretion rate as

$$\dot{M}_{\rm Edd} = L_{\rm Edd}/\left(\eta c^2\right) = L_{\rm Edd}/\left(0.057 c^2\right)\,. \tag{2}$$

In equation (2), η denotes the radiative efficiency of accretion, which we set to the thin disc value in the Schwarzschild metric, $\eta = 0.057$ (Novikov & Thorne 1973), as a unit convention defining $\dot{M}_{\rm Edd}$.

The actual radiative efficiency in the simulated accretion process, defined through

$$\eta = L/\left(\dot{M} c^2\right), \tag{3}$$

can be determined by computing $\dot{M}$ through the horizon and L through a fiducial surface. Note that in the presence of advection sphere-integrated luminosity may not be equal to the integrated radiative power produced locally in the disc, causing some additional ambiguity in the efficiency definition. In Lančová et al. (2019), we reported $L = 0.36 L_{\rm Edd}$ for $\dot{m} = 0.6$, measured in the GRRMHD simulation. This implied a significant decrease of radiative efficiency with respect to the NT disc, which we interpreted as a consequence of advection, prominent in the simulation. With the post-processed radiative transfer, we found, somewhat surprisingly, the efficiency of a sub-Eddington puffy disc in the Schwarzschild metric to be consistent with that of the NT disc within the measurement uncertainties. While the discrepancy may be partly explained with the imperfections of the luminosity measurement in the GRRMHD simulation (we integrated the radiative flux over a $25\,M$-radius sphere in the optically thin region, ignoring contributions from larger radii or optically thick outflows), we currently suspect that this is related to limitations of the M1 closure scheme for the radiation tensor employed in KORAL (Sądowski et al. 2013). Under the M1 approximation, radiation propagates in a single direction in the optically thin regime, and a large part of the radiation released in the inner flow consequently appears to be swallowed by the black

[1] Apart from simulations, fully two- or three-dimensional (analytical) solutions for accretion discs have been obtained only for α-discs (e.g. Kluzniak & Kita 2000; Regev & Gitelman 2002).

[2] https://github.com/achael/koral_lite

[3] The Eddington luminosity is defined as $L_{\rm Edd} = 4\pi c\, GMm_{\rm H}/\sigma_{\rm T} = 1.26 \times 10^{38}\,(M/M_\odot)$ erg s^{-1}, where G is the gravitational constant, c is the speed of light, M is the mass of the gravitating body, $m_{\rm H}$ and ${\rm M}_\odot$ are the hydrogen atom and solar masses, respectively, and $\sigma_{\rm T}$ is the Thompson cross-section.

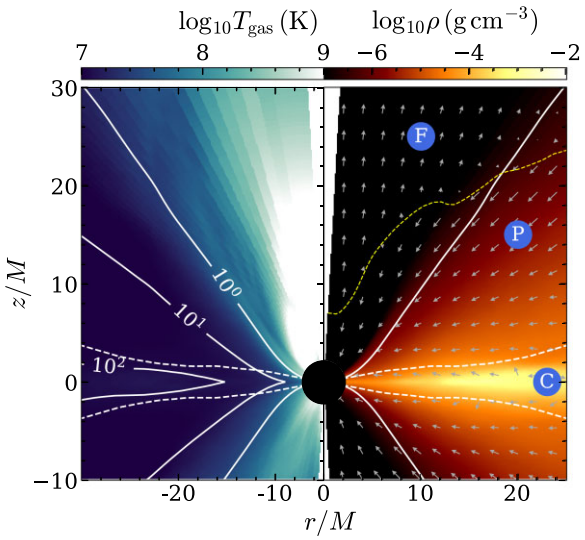

Figure 1. Structure of a puffy disc. The white dashed line in both panels indicates the vertical thickness (density scale height) of the dense disc core (region C). Left: Gas temperature $T_{\rm gas}$ with contours of the optical depth $\tau = 1$ (photosphere, separating regions P and F), $\tau = 10$, and $\tau = 100$ (white continuous lines). Right: Gas density map; arrows indicate the gas velocity in the r–θ plane. The white contour denotes the position of the photosphere ($\tau = 1$) and the dashed yellow line indicates the border between the inflowing (below) and outflowing (above) regions.

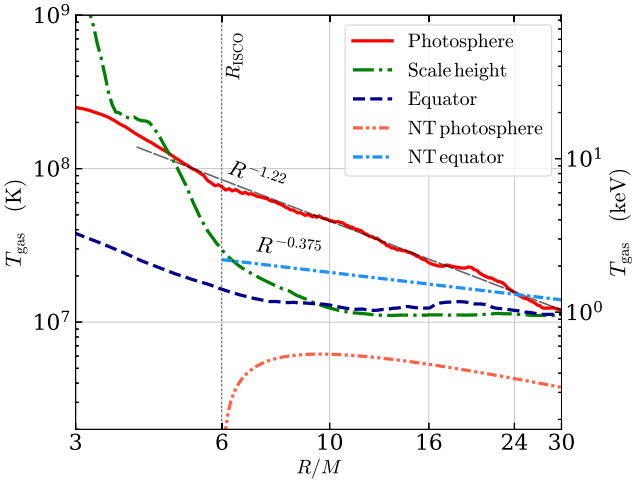

Figure 2. Radial profiles of temperature in the $\dot{m} = 0.6$ puffy disc for the equatorial plane, disc core scale height, and the photosphere. The photospheric temperature is reasonably well approximated as a power law of the cylindrical radius R with an exponent (p) of -1.22. The disc core heats up predominantly very close to the black hole, with slow temperature variations for $R > R_{\rm ISCO}$. Analytical NT disc temperature profiles for the same system parameters are shown for comparison.

hole in the GRRMHD simulation, whereas it may possibly escape to infinity when a more general radiative transfer problem is solved with HEROIC.

2.2 Properties of puffy discs

Our numerical simulations predict a stratified structure in a mildly sub-Eddington accretion disc. In Fig. 1, we indicate three zones of the emerging geometry. The zone denoted by C represents the high-density core of the disc, with a density scale height thickness (h/r) of ∼0.1, which contains most of the gas. It is supported above the mid-plane of the disc primarily by magnetic pressure that dominates over radiation pressure, and both strongly dominate over gas pressure (Lančová et al. 2019). The white dashed line in Fig. 1 shows the density scale height of the disc core. Zone P corresponds to the puffy region. While being optically thick to scattering and delimited by the photosphere at $h/r \sim 1$ (white solid line in the right-hand panel of Fig. 1), this region is characterized by a gas density that is about two orders of magnitude lower than that in the disc core. The gas in the puffy region is vigorously accreting on to the black hole. The turbulent dissipation heats up the puffy region and the temperature reaches several times 10^7 K at the photosphere (see Fig. 2).

In comparing various disc models, it is convenient to model the temperature as a power-law function of the cylindrical radius R (Kubota & Makishima 2004). In the puffy disc, the radial temperature dependence varies from layer to layer in the different zones of the accreting structure. The photospheric temperature scales as $R^{-1.2}$ (see Fig. 2). While this is significantly steeper than for an NT disc, where $T \propto R^{-0.75}$ (Novikov & Thorne 1973; Shakura & Sunyaev 1973; Page & Thorne 1974), the photosphere (surface of last scattering) of a puffy disc is also much hotter in the inner disc region than the NT disc surface. Moreover, the puffy disc photosphere extends below the innermost stable circular orbit (ISCO; $R = 6M$ for the Schwarzschild space–time) with a consistent continuation of the power-law temperature dependence, whereas NT surface temperature drops to zero at ISCO. The temperature of the disc core, both in the equatorial plane and at the density scale height, grows rapidly in the plunging region ($R < R_{\rm ISCO}$) as a consequence of vertical compression, but changes more slowly with radius for $R > R_{\rm ISCO}$. As can be seen in Fig. 2, these temperature profiles are lower but comparable with the NT disc equatorial temperature $T \propto R^{-0.375}$ for $R > R_{\rm ISCO}$. At $R > 15M$, optically thick outflows from the outer layer of the puffy zone develop (see the right-hand panel of Fig. 1). The third zone, denoted by F in Fig. 1, is a low-density, low-optical depth, hot (10^8–10^9 K) funnel zone. The optically thin material in the funnel, driven by collimated radiation, is outflowing above the stagnation surface located at $z \approx r + 7M$.

The morphology of the puffy disc is somewhat similar to the predictions of Zhang et al. (2000) based on X-ray spectral modelling of BHXBs, and of Begelman & Pringle (2007), based on arguments about active galactic nucleus discs. Conclusions similar to ours about the vertical structure of the disc, including the importance of magnetic pressure, have been reached by Mishra et al. (2020), based on non-relativistic simulations.

3 BEAMING AND OBSCURATION

The presence of an optically and geometrically thick puffy region has important consequences for the radiative output received by the observer. We illustrate this in Fig. 3, where ray-traced bolometric (frequency-integrated) images of puffy accretion discs (computed with HEROIC; Narayan et al. 2016) are contrasted with NT thin disc images (computed with GYOTO; Vincent et al. 2011) for several inclinations θ. For the thin disc, no vertical structure was assumed. While there seem to be no perspectives in the foreseeable future

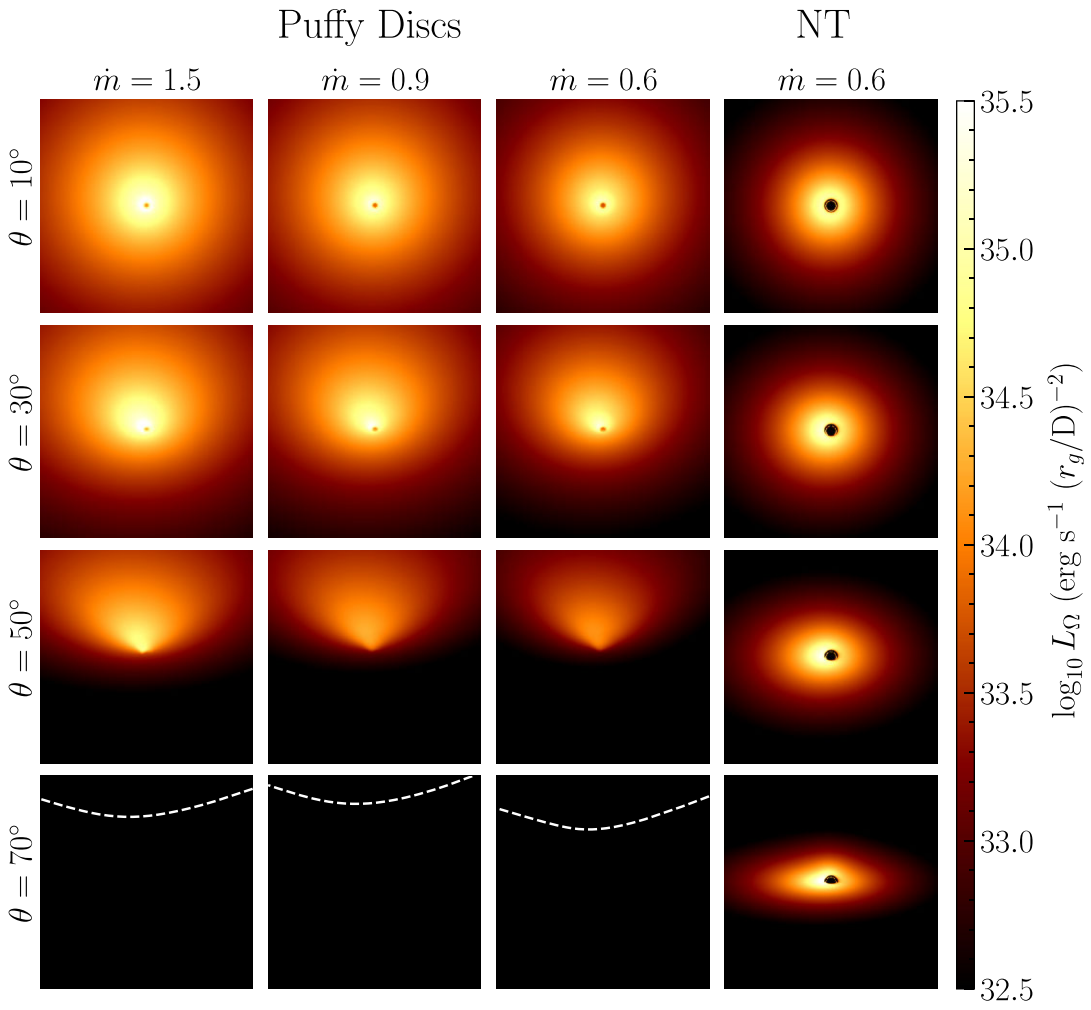

Figure 3. Puffy disc appearance given as L_Ω, frequency-integrated isotropic luminosity per solid angle $(r_g/D)^2$, where $r_g = GM/c^2$ and D represents the observer's distance to the source, using $M = 10\,\mathrm{M}_\odot$, and $D = 10$ kpc. We show puffy disc images computed for different inclinations θ, for mass accretion rates of 1.5, 0.9, and 0.6 $\dot{M}_{\mathrm{Edd}}$ (*first three columns*), compared to the NT disc of 0.6 $\dot{M}_{\mathrm{Edd}}$ (*last column*). The white dashed lines in the bottom row of the puffy disc images correspond to 10^{31} erg s$^{-1}(r_g/D)^{-2}$ contours – at the inclination of 70°, the inner disc is no longer visible in the images. All results were computed in the Schwarzschild metric and correspond to the $\left(240\,r_g/D\right)^2$ field of view.

of observing resolved structures of accretion discs in BHXBs,[4] this exercise is very helpful in recognizing the influence of inclination and elucidating differences between the NT thin disc and the GRRMHD puffy disc solutions. At low inclinations ($\theta \leq 30°$), observers see the puffy disc system through the low-optical depth funnel region. The radiation then becomes collimated in the funnel surrounded by the geometrically and optically thick puffed-up accretion disc in a way similar to the classic analytical thick disc solutions (Abramowicz, Jaroszynski & Sikora 1978), and it is enhanced by the reflections from the optically thick funnel walls (Sikora 1981). These effects are self-consistently handled by the HEROIC code. Notice that the mostly purely geometrical beaming effect discussed here is different from relativistic beaming (the Doppler effect related to the emitter approaching with a relativistic velocity), as observed in jets. The latter has relatively little importance in the case of puffy discs, since the outflowing gas inside the funnel has a velocity of only $\sim 0.1\,c$ and a very low density.

The luminosity, L, is computed directly from the simulated spectra, at a fiducial distance D:

$$L = 2\pi D^2 \int_0^\pi \left(\int_0^\infty F_\nu \,\mathrm{d}\nu\right) \sin\theta \mathrm{d}\theta \tag{4}$$

$$= \tfrac{1}{2} \int_0^\pi \left(\int_0^\infty L_\nu \,\mathrm{d}\nu\right) \sin\theta \mathrm{d}\theta \,. \tag{5}$$

The collimation of radiation in the funnel causes an increase of the so-called isotropic luminosity, L_{iso}, that would be inferred from observations at particular inclination θ, with

$$L_{\mathrm{iso}} = 4\pi D^2 F = \int\limits_{\mathrm{image}} L_\Omega \,\mathrm{d}\Omega = \int\limits_0^\infty L_\nu \,\mathrm{d}\nu \,. \tag{6}$$

At the axis ($\theta = 0$), the increase corresponds to a factor of $1/b = L_{\mathrm{iso}}/L$ relative to the actual luminosity (e.g. King et al. 2001). In equation (6), $F = \int F_\nu \mathrm{d}\nu$ is the flux seen by the observer at distance D. In fact, the flux F_ν, luminosity per solid angle L_Ω, and luminosity per frequency L_ν all depend on the observer's inclination θ, as can

[4]The field of view of panels in Fig. 3 corresponds to 2.4 ns of arc, four orders of magnitude less than the highest resolution achieved by global radio-interferometric arrays (EHT Collaboration 2019).

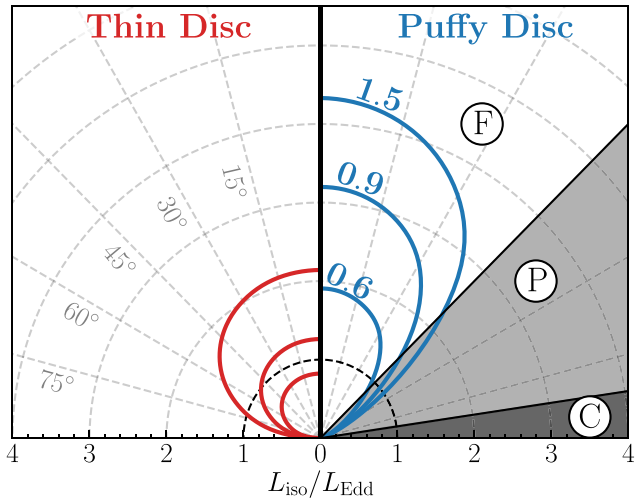

Figure 4. Bolometric beaming pattern comparison between a puffy disc and the NT thin disc, for mass accretion rates of 0.6, 0.9, and 1.5 $\dot{M}_{\rm Edd}$ and spin $a_* = 0$. Puffy discs collimate radiation along the axis of symmetry with a beaming factor $b \approx 0.3$, and the radiation is strongly attenuated for large inclinations.

be seen in Fig. 3, and thus $L_{\rm iso}$ is a function of the same angle (see Fig. 4).

In our simulations, we measure a puffy disc beaming factor of $b \approx 0.25$–0.30, without a strong indication of dependence on $\dot{m}$, as the general three-zone puffy disc structure does not change much between $\dot{m} = 0.6$ and 1.5. The lack of dependence of the beaming factor on the mass accretion rate contradicts the $b \propto \dot{m}^{-2}$ relation expected from King (2009), which was derived on the assumption that the disc height increases with the mass accretion rate. We attribute this discrepancy to the roughly constant h/r ratio (regardless of the accretion rate), which is related to advection limiting the growth of the disc thickness with $\dot{m}$ (Lasota et al. 2016; Wielgus et al. 2016).

At inclination $\theta = 10^\circ$, Fig. 3 shows that puffy and NT discs are similar in appearance; however, the puffy disc is brighter overall because of the beaming effect. Because of the low optical depth in the funnel, even the innermost region of the accretion flow in the immediate vicinity of the event horizon is visible (the central dark spot in the puffy disc images). This central gap in the image is much more prominent in the NT model, in which radiation is only emitted at radii larger than the ISCO. At larger inclinations, a different effect starts to be relevant – the puffed-up optically thick disc starts to obscure the view of the inner part of the accretion flow. In Fig. 3, we see that at an inclination of 50° the puffy disc image is already dominated by the funnel wall opposite to the observer, with the core of the system obscured. At 70° inclination, the inner regions of the puffy disc are not visible and the radiative flux decreases by about two orders of magnitude. At the same time, the impact of the inclination on the NT disc appearance is much less prominent, as the disc remains geometrically thin, supporting neither efficient beaming nor obscuration effects.

Interestingly, the development of an elevated disc structure during the high mass accretion rate phase has been proposed as an interpretation of the X-ray spectra of the large inclination source V404 Cygni (Motta et al. 2017). The enhanced complexity of the X-ray outburst light curves of high-inclination sources was also identified as hinting at a time-variable obscuration (Narayan & McClintock 2005). Although low-luminosity numerical solutions of stable disc are not yet available, we imagine that a disappearance of the puffy region, and transition between a thin and a puffy disc geometry, may occur at some accretion rate, perhaps at $\sim 0.3\dot{M}_{\rm Edd}$.

We further quantify the collimation / obscuration effects in Fig. 4, where we compare the beaming pattern of NT thin discs and puffy discs for the mass accretion rates of $\dot{m} = 0.6$, 0.9, and 1.5. In general, beaming is maximal at low inclinations and decreases for higher viewing angles and the beaming factor does not strongly depend on the mass accretion rate. The face-on inclination 'beaming' factor[5] of the NT disc is $b_{\rm NT} \approx 0.7$, which corresponds to an effect about 2.5 times less prominent than in the case of the puffy disc. Hence, an NT disc with a mass accretion rate of $1.5\dot{M}_{\rm Edd}$ appears as a $2.1L_{\rm Edd}$ luminosity source when viewed along the axis. A puffy disc of the same mass accretion rate, however, implies an isotropic luminosity of $4.4L_{\rm Edd}$.

A mildly sub-Eddington puffy disc system viewed at low inclination would be conventionally classified as an ultraluminous X-ray source (ULX; Kaaret, Feng & Roberts 2017). We have already noted in Section 2.1 that for sub-Eddington accretion, the puffy disc luminosity is proportional to the mass accretion rate; that is, the efficiency does not change appreciably with $\dot{m}$ for $\dot{m} \leq 1.5$. Assuming approximate proportionality also between luminosity and black hole mass (with the caveat that, in fact, radiative simulations do not strictly scale with the mass of the black hole), we could give an approximate formula for beamed observed isotropic luminosity of a puffy disc:

$$L_{\rm iso} \sim 5 \times 10^{39} \left(\frac{M}{10\,{\rm M}_\odot}\right) \left(\frac{\dot{M}}{\dot{M}_{\rm Edd}}\right) \left(\frac{b}{0.25}\right)^{-1} \frac{\rm erg}{\rm s}. \quad (7)$$

This may allow an interpretation of those ULXs that comprise a BHXB in the puffy disc accretion framework.

4 SPECTRAL PROPERTIES OF PUFFY DISCS

Traditionally, BHXBs and ULXs are studied with phenomenological models, i.e. by composing a total model from as many components as needed to emulate the observed spectrum: a thin disc, a corona, an iron line, a reflection bump, etc. Given the comparatively simple and analytical nature of the model components, this has the crucial advantage that it allows to identify and characterize different disc properties and effects very efficiently. However, different underlying disc structures necessarily modify the contribution of other components, and this can lead to a misreading of the importance of added effects. Within the GRRMHD framework, we can self-consistently solve for the structure of the accretion system, taking into account the radiation feedback, influence of the magnetic field, vertical stratification, and outflows. All these effects influence the spectra in a highly non-trivial and non-linear way that cannot be fully reproduced by adding and/or multiplying a series of analytical model components. Synthetic spectra from GRRMHD simulations of hard state BHXBs were recently discussed by Dexter, Scepi & Begelman (2021).

We present synthetic puffy disc spectra computed using the HEROIC code in Figs 5–6. In the left-hand panel, we explore the influence

[5]In reality, for the thin disc the beaming pattern is related to the usual non-isotropic emission from the photosphere, the flux decreasing with increasing inclination angle. The unrelated effect of Doppler beaming affects the NT spectra at large viewing angles.

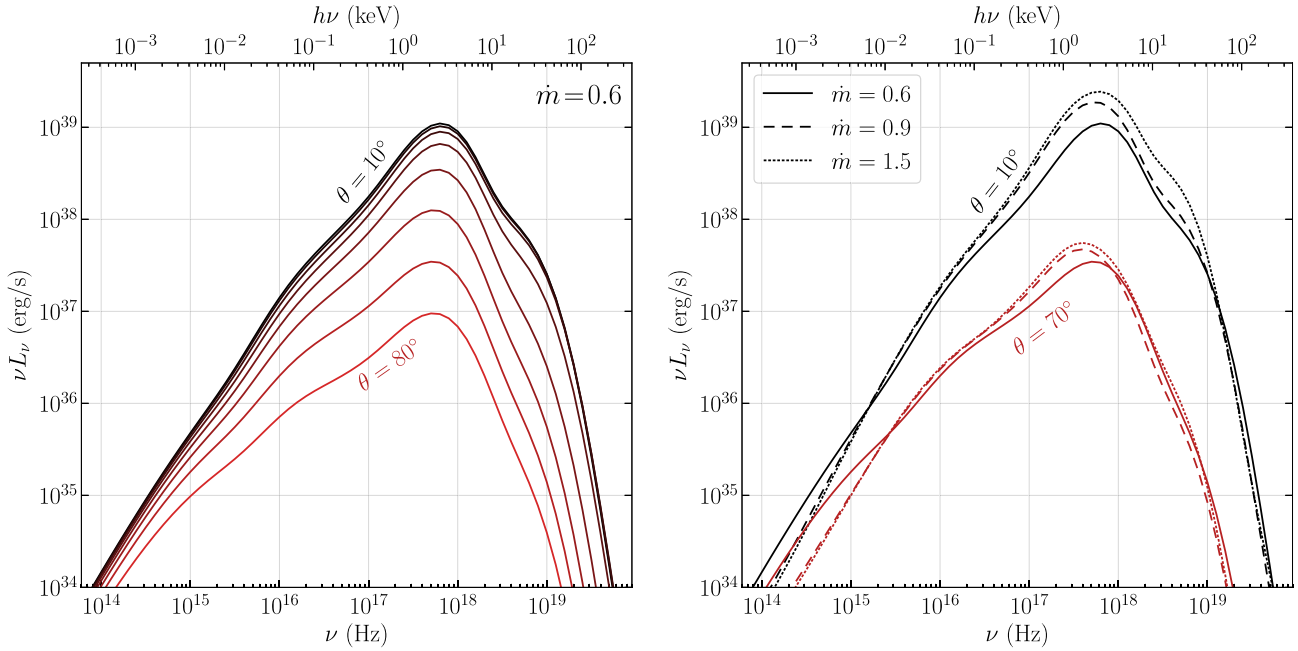

Figure 5. Properties of puffy disc spectra for an $M = 10\,\mathrm{M}_\odot$ black hole. *Left:* isotropic radiative power per logarithmic frequency interval, as a function of the observer's inclination, from 10° (nearly face-on) to 80° (nearly edge on). Right: isotropic radiative power per logarithmic frequency interval for three GRRMHD simulations, corresponding to different mass accretion rates $\dot{m}$.

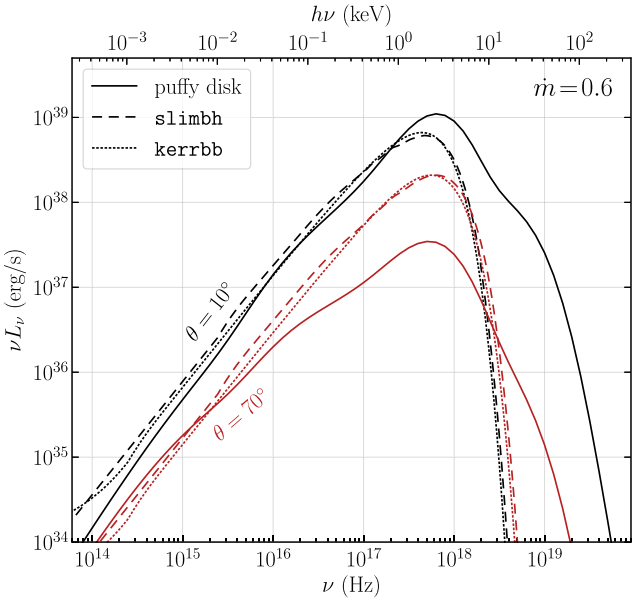

Figure 6. Comparison of puffy disc spectra to multicolour blackbody spectra of thin (`kerrbb`) and slim (`slimbh`) disc models of the same mass $M = 10\,\mathrm{M}_\odot$, mass accretion rate $\dot{m} = 0.6$, and observer's inclination θ.

of the inclination, expanding on the total luminosity discussion from Section 3. The inclination θ has a strong impact on the puffy disc spectra because of the beaming at low inclinations and obscuration at high inclinations. Between $\theta = 10°$ and 80°, the maximum value of the spectral energy distribution (SED) changes by two orders of magnitude. However, the location of the spectral peak is only mildly affected, and remains around 3 keV. At low inclinations, the SED develops a hump at around 20 keV, related to the Comptonized radiation produced in the innermost part of the accretion flow.

The right-hand panel of Fig. 5 explores the differences between our three GRRMHD simulations for a range of mass accretion rates and two specific inclinations. Apart from total radiative output scaling, they indicate similar features. A small shift of the peak towards higher energies is visible in the $\dot{m} = 0.6$ model. This is related to the lower optical depth of the system.

Finally, in Fig. 6 we contrast the puffy disc spectra with those of a thin NT disc and a slim disc in their XSPEC implementations (`kerrbb` and `slimbh`, respectively). These are two relativistic, height-integrated α-disc models are based on Novikov & Thorne (1973) and Sądowski (2009), respectively. They both assume a geometrically thin and optically thick disc that consists of a sum of annular blackbody emitters. This allows one to determine the total disc luminosity by radially integrating $L(r) \propto T_{\mathrm{eff}}^4(r)$. Both models parametrize the turbulent viscosity by assuming stress to be proportional to pressure via a constant α (Shakura & Sunyaev 1973). The slim disc differs from the thin NT disc on account of its additional advective cooling that transports an increasing fraction of the disc thermal energy towards the black hole as the mass accretion rate rises.

Slim and thin disc spectra appear similar at the moderate accretion rate of $0.6M_{\mathrm{Edd}}$. Neither of them accounts for Compton scattering that can be modelled separately (see Section 5). This causes a difference with respect to the puffy disc, where Comptonization is self-consistently accounted for.

For intermediate inclinations, around $\theta = 48°$, where neither beaming nor obscuration is dominant, the puffy disc peak of SED is similar to that of the NT disc model. The comparison between NT and puffy disc spectra at $\theta = 48°$ is shown in Fig. 7. There is a deficit of power in the puffy spectrum with respect to the NT disc in the range of 0.1–1.0 keV and an excess of puffy disc power above 3 keV. The puffy disc spectrum above 10 keV is described reasonably well by a power law with a νL_ν slope equal to -2, corresponding to a photon index $\Gamma = 4$.

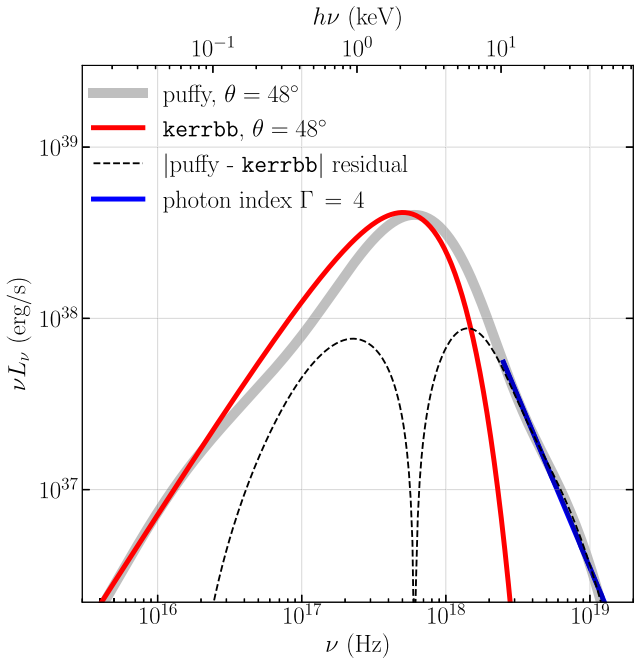

Figure 7. Comparison of NT `kerrbb` (red lines) and puffy disc (grey lines) spectra at an intermediate inclination of $\theta = 48^\circ$ for a mass accretion rate $\dot{m} = 0.6$. The absolute value of the difference between the models is shown by dashed lines. In the range of 10–40 keV, the puffy disc spectrum can be approximated with a power law corresponding to a photon index $\Gamma = 4$ (blue line).

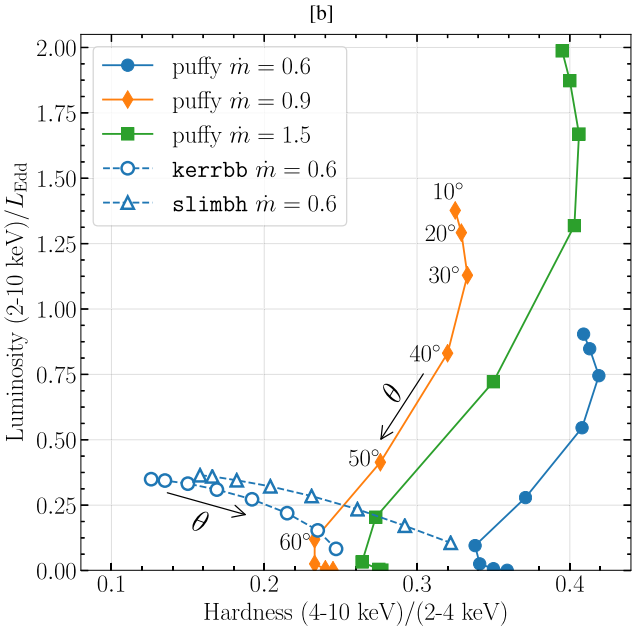

Figure 8. Luminosity–hardness diagram for the synthetic puffy disc spectra. Vertical axis represents the 2–10 keV-band isotropic luminosity in the Eddington units. Hardness is defined as the ratio of photon counts in the 4–10 and 2–4 keV bands. For comparison, the location of the `kerrbb` and `slimbh` spectra for $\dot{m} = 0.6$ is shown as well; for small and moderate inclinations, they both indicate less luminous and softer spectra than a puffy disc at the same mass accretion rate.

The effect of inclination on the luminosity and hardness of the spectra for different disc models is shown in Fig. 8. As discussed in Section 3, the observer's inclination has a huge impact on the observed puffy disc luminosity. The hardness of puffy disc spectra diminishes between 30° and 60° inclination because of the obscuration of the inner (beamed hard X-ray) region of the disc. In comparison, both the thin and slim discs are very soft at low inclinations as they completely lack the hard Compton component. They become harder under increasing viewing angles due to relativistic beaming in directions close to the plane of the disc, primarily affecting the inner region of the disc (e.g. Kulkarni et al. 2011). Moreover, at $\dot{m} = 0.6$ slim disc spectra tend to be harder than those of an NT thin disc, owing to advection that traps thermal energy in the disc, transports it inwards, and releases it at smaller radii as harder emission. The non-monotonic relation between the spectral hardness and mass accretion rate for the puffy discs, seen in Fig. 8, is more difficult to understand and can be attributed to an interplay between the temperature of the disc, which depends on the mass accretion rate, and the obscuration.

5 MODELLING PUFFY DISC SPECTRA

During their outbursts, X-ray binaries pass a series of different disc states and typically spend a comparatively long time in a highly luminous, disc-dominated state with a characteristic blackbody-dominated SED. Strictly thermal-dominated spectra, i.e. spectra with a disc-to-total flux fraction of above 75 per cent (in the energy range of 2–20 keV), a weak non-thermal power continuum, and very weak variability (rms $<$ 1 per cent), can be used to extract the black hole spin (continuum-fitting method; e.g. Remillard & McClintock 2006; Done et al. 2007; McClintock et al. 2014).

If we were to observe spectra from an astrophysical object consistent with our puffy disc model, how would they be interpreted by the standard spectral fitting tools? To address this question, we generated synthetic test spectra from a puffy disc simulation in the energy range of 0.1–100 keV, and fitted them with the XSPEC software package (Arnaud 1996). The synthetic puffy spectra correspond to a GRRMHD simulation of a Schwarzschild black hole of spin $a_* = 0$, mass accretion rate $\dot{m} = 0.6$ (as defined in equation 1), and mass $M = 10\,\mathrm{M}_\odot$, at a distance $D = 10\,\mathrm{kpc}$, seen from two different inclinations, $\theta = 10^\circ$ and 60°. We fit these spectra with a fully relativistic (including gravitational bending of photon trajectories) thin disc model, `kerrbb` (Li et al. 2005), and a fully relativistic, advective slim disc model, `slimbh` (Sądowski 2009; Straub et al. 2011). Each disc component is accompanied by a thermal Comptonization component `nthcomp` (Zdziarski, Johnson & Magdziarz 1996; Życki, Done & Smith 1999) that accounts for seed photons originating in the disc that are upscattered to higher energies by a homogeneous corona.

For each disc model, the dynamical BHXB parameters, namely mass M, distance D, and inclination θ, are assumed to be known and fixed, while the black hole spin a_* and total (spherically integrated, inclination-independent) disc luminosity L_{disc} (in `kerrbb`, equivalently, the mass accretion rate) are fitted for. The viscosity parameter is fixed at $\alpha = 0.1$ in each model. In the Compton component, the temperature of the seed photons, T_{bb}, and the electrons in the corona, T_{e}, as well as the photon index, Γ, are fitted for. Usually, in order to reduce the number of free parameters, T_{bb} is fixed at some 'reasonable' value. Here, we leave it free to assess how well the T_{bb} parameter matches the puffy disc temperature, as presented in Fig. 2.

Given the phenomenological nature of the models, they are both able to fit the puffy disc spectra with high fidelity (low χ^2 per degree of freedom, χ^2/dof), as shown in Fig. 9 and Table 1. We assumed a 10 per cent error budget on the simulated spectral measurements. While the fits are well behaved, the models formally overfit our

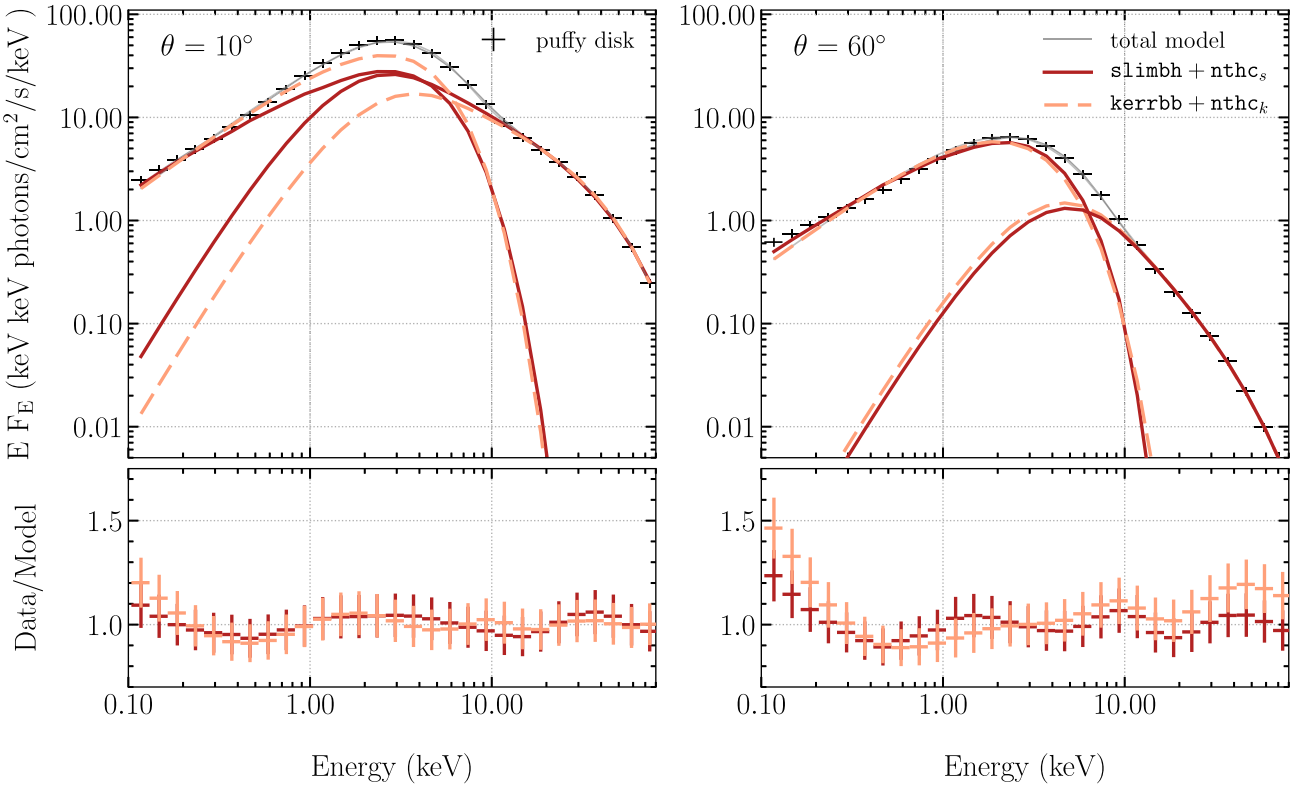

Figure 9. Synthetic puffy disc spectra fitted by standard XSPEC models. The synthetic puffy disc spectra (black crosses) are calculated for a hypothetical BHXB at $D = 10$ kpc, with a black hole mass $M = 10\,M_\odot$, a mass accretion rate $\dot{m} = 0.6$, and inclinations $\theta = 10°$ (left-hand panel) and $\theta = 60°$ (right-hand panel). They are fitted with a disc model plus a Compton component: `slimbh` + `nthcomp`$_s$ (solid lines) and `kerrbb` + `nthcomp`$_k$ (dashed lines).

Table 1. XSPEC fits to synthetic puffy disc spectra with $a_* = 0$ and $\dot{m} = 0.6$. Each of the disc models, `slimbh` and `kerrbb`, is accompanied by the thermal Comptonization model `nthcomp`.

	Puffy $\theta = 10°$		Puffy $\theta = 60°$	
	`slimbh`	`kerrbb`	`slimbh`	`kerrbb`
a_*	$0.82^{+0.08}_{-0.16}$	$0.86^{+0.08}_{-0.14}$	$0.55^{+0.11}_{-0.29}$	$0.48^{+0.12}_{-0.41}$
$L_{\rm disc}/L_{\rm Edd}$	$0.73^{+0.15}_{-0.16}$	$0.79^{+0.1}_{-0.1}$	$0.21^{+0.19}_{-0.24}$	$0.17^{+0.05}_{-0.03}$
Γ	$2.85^{+0.17}_{-0.20}$	$2.72^{+0.24}_{-0.24}$	$3.62^{+0.27}_{-0.29}$	$3.67^{+0.34}_{-0.27}$
$T_{\rm e}$ (keV)	$14.95^{+5.31}_{-2.68}$	$13.05^{+4.62}_{-2.43}$	$19.51^{+17.34}_{-5.75}$	$19.26^{+21.81}_{-5.58}$
$T_{\rm bb}$ (keV)	$0.50^{+0.08}_{-0.07}$	$0.67^{+0.22}_{-0.15}$	$1.01^{+0.57}_{-0.31}$	$0.97^{+0.48}_{-0.29}$
χ^2/dof	9.32/29	8.51/29	11.58/29	27.97/29

simulated data due to the assumed uncertainties. Nevertheless, the fits demonstrate that all quantities can be well constrained. Furthermore, typical values for BHXBs are obtained, albeit with results that are quite different from the true values of $a_* = 0$ and $\dot{m} = 0.6$.

The highly beamed low-inclination ($\theta = 10°$) puffy spectrum is preferentially fitted with a high black hole spin $a_* \approx 0.7$–0.8 for both disc models, and a (thermal) disc luminosity that is slightly higher than the true luminosity of the puffy disc, but much lower than its isotropic luminosity at this inclination angle. The Comptonization component fits a photon index (Γ) of about 2.8, a disc temperature ($T_{\rm bb}$) of $\approx$0.6 keV, and an electron temperature ($T_{\rm e}$) of approximately 14 keV. While the thin and slim disc models require a cranked up spin parameter to fit the low-energy part of puffy spectra, the Compton model recovers the shape of the high-energy emission with typical values for a warm corona (see e.g. Różańska et al. 2015). The dim, inclined puffy disc ($\theta = 60°$) is fitted with moderate black hole spins and very low disc luminosities, combined with a warm corona of $\Gamma \approx 3.6$, $T_{\rm bb} \approx 1$ keV, and $T_{\rm e} \approx 19$ keV.

The measurement of spin is impaired by the large Compton contributions, which is a known obstacle to the continuum-fitting method and one of the reasons why only the strictly thermal-dominated states can be effectively used to measure black hole spins, as pointed out by e.g. Gierliński & Done (2004), Done & Kubota (2006), McClintock et al. (2006), and Middleton et al. (2006). Only limited attempts have been made to extend the continuum-fitting method towards modelling spectra with an appreciable power-law component (e.g. Steiner et al. 2009).

In Table 1, we show the parameters of the best fits with uncertainties corresponding to 90 per cent confidence intervals. The classical disc models gravely overestimate the black hole spin, with respect to $a_* = 0$ that was assumed in the underlying GRRMHD simulation. This overestimate reflects the high temperatures in the puffy disc, seen in Fig. 2. The mass accretion of the fitted models corresponds to $\dot{m} \approx 0.4$ for low inclination and $\dot{m} \approx 0.1$ for large inclination (with $\dot{m}$ defined using the zero-spin efficiency convention from equation 1); i.e. the fitted $\dot{M}$ value is only equal to 2/3 and 1/6, respectively, of the true value in the simulation. The mismatch with respect to the true value of $\dot{m} = 0.6$ is explained by the increased disc efficiency at high black hole spin, while the variation of the fitted mass accretion rate with the inclination angle involves beaming/obscuration effects as well.

Puffy disc spectra do not describe the strictly thermal-dominated state in BHXBs; they are not strongly dominated by thermal radiation but comprise a considerable amount of Compton up-scattered photons (see Fig. 5). Their global (0.1–100 keV) blackbody-to-total

flux ratio, as measured by XSPEC's thin and slim disc models, lies for $\theta = 10^\circ$ at 54 per cent and for $\theta = 60^\circ$ at 83 per cent, whereas in the 2–20 keV range the disc contribution is just 44 and 72 per cent, respectively. In combination with their rather steep high-energy slopes (see Γ in Table 1) and high normalizations, these properties can be related to the spectra observed in two accretion disc states. On the one hand, they resemble the so-called intermediate states in BHXBs. These are complex states associated with transitions between the hard and soft states and the occurrence of quasi-periodic variability (Méndez & van der Klis 1997; Remillard & McClintock 2006). Although puffy discs can exhibit, depending on the viewing angle, a considerably larger (even super-Eddington) apparent luminosity than average BHXBs, a spectral resemblance is expected due to the presence of a Comptonized corona. On the other hand, puffy disc spectra show morphological similarities to certain ULXs, namely those that show a soft ultraluminous state. There is increasing evidence that at least some ULXs are powered by accreting stellar-mass black holes that produce three specific types of ultraluminous disc states: a single-peaked broadened ultrasoft disc, a two-component hard ultraluminous state, and a soft ultraluminous state. The last one is typically described as a cool disc with a warm corona component (see Gladstone, Roberts & Done 2009; Sutton, Roberts & Middleton 2013; Mondal et al. 2021), which resembles our puffy disc spectra.

6 DISCUSSION

In this paper, we discussed the observational signatures, and in particular the spectra, of the puffy disc – a numerical model of stable accretion in the range of luminosities (currently) above $0.5L_{\rm Edd}$. Unlike Narayan et al. (2017) or Ogawa et al. (2021), who treated a strongly super-Eddington case, we focused on mildly sub-Eddington accretion. This is the regime where standard geometrically thin disc models fail to correctly predict the observed source spectra, which happens at luminosities above $0.3L_{\rm Edd}$. The puffy disc solution captures the physics of such luminous accretion flows. In our approach, radiation is incorporated into the GRRMHD simulations, allowing for a self-consistent development of a vertically stratified, magnetic and radiation pressure-dominated, accretion structure. A low-density 'puffy' region, Keplerian, rapidly accreting, and geometrically and optically thick, develops above the denser disc core zone; spectroscopically, it resembles a 'warm corona'.

The observable luminosity of puffy discs depends much more strongly on the observer's inclination to the system axis than is the case for standard geometrically thin disc models. At high inclinations, the emission is obscured by the geometrically thick corona blocking the view of the central region of the disc. The development of an obscuring geometrically thick structure during the luminous thermal state may explain unusual variability of BHXB sources, e.g. V404 Cygni. At low inclinations, the emission is geometrically collimated by the puffy region, increasing the observed radiative flux. Such a strong beaming effect is absent in thin discs, and may be relevant for the interpretation of at least some ULX sources.

We investigated synthetic spectra of puffy discs and attempted to fit them with standard fitting models available in XSPEC. We found that a Comptonized NT disc fits the puffy disc spectra well in terms of the statistical fit quality metrics. However, for our model of a non-spinning black hole the currently available fitting tools erroneously find a large positive spin value. This offers a theoretical interpretation for known problems with fitting BHXB spectra in luminous states, although we cannot currently provide a quantitative characterization of these effects in the Kerr metric. For instance, for LMC X-3 Straub et al. (2011) and Steiner et al. (2014) reported that the spin estimate of $a_* \approx 0.21$ decreases with luminosity due to the incompleteness of physical models (lack of Comptonization) at luminosities larger than about $0.3L_{\rm Edd}$. For the Schwarzschild puffy disc solution, we can only see an increase of the spin estimate with respect to the ground truth value of $a_* = 0$, and indeed this is what happens as the standard XSPEC models try to emulate the puffy disc spectra by tuning the free parameters.

The puffy spectra resemble intermediate states between soft and hard emission states of BHXBs. The complex intermediate states are associated with quasi-periodic variability and there currently exists no established accretion disc model to describe these states. We have demonstrated that numerically calculated puffy disc spectra, which self-consistently model accretion discs with a significant Comptonized atmosphere (warm corona), could qualitatively describe these intermediate states. It remains to be seen whether the GRRMHD framework could provide a quantitatively correct interpretation of the real astrophysical sources, extending the region of applicability of the continuum-fitting spin estimation method.

It is currently computationally too expensive to produce a fine-mesh grid in the parameter space of puffy discs, to calculate a table model that could be implemented for public use in the XSPEC software package. For this reason, we cannot at present explicitly fit puffy disc models to observational X-ray spectra. However, this is clearly one of the directions that should be pursued in the future. Currently, we do not have puffy disc solutions for the Kerr metric with $a_* \neq 0$, nor for $L < 0.6L_{\rm Edd}$. The latter solutions are urgently needed, as there as yet exist no known stable solutions for disc accretion at rates corresponding to the luminosity of many BHXB sources.

ACKNOWLEDGEMENTS

The authors thank Andrew Chael, Brandon Curd, and Aleksander Sądowski for support with the KORAL code, as well as Silke Britzen, Michal Bursa, and Monika Mościbrodzka for valuable comments and discussions. The computations in this work were supported by the PLGrid Infrastructure through which access to the Prometheus supercomputer, located at ACK Cyfronet AGH in Kraków, was provided. This work was supported in part by the Polish NCN grant 2019/33/B/ST9/01564 and the Black Hole Initiative at Harvard University, which is funded by grants from the John Templeton Foundation and the Gordon and Betty Moore Foundation to Harvard University. MA acknowledges the Polish NCN grant 2015/19/B/ST9/01099, while AR acknowledges the NCN grant 2021/41/B/ST9/04110. MA and GT acknowledge the Czech Science Foundation grant GX21-06825X, and DL acknowledges the internal grant of SU SGS/13/2019 and the Student Grant Foundation of the Silesian University in Opava, grant number SGF/1/2020, which has been carried out within the EU OPSRE project entitled 'Improving the quality of the internal grant scheme of the Silesian University in Opava', reg. number CZ.02.2.69/0.0/0.0/19_073/0016951. RN acknowledges the support of the NSF grants OISE-1743747 and AST-1816420. We also thank Alexandra Elbakyan for her contributions to the open science initiative.

DATA AVAILABILITY

The data underlying this article will be shared on reasonable request to the corresponding author.

REFERENCES

Abramowicz M. A., Fragile P. C., 2013, Living Rev. Relativ., 16, 1
Abramowicz M., Jaroszynski M., Sikora M., 1978, A&A, 63, 221
Abramowicz M. A., Czerny B., Lasota J. P., Szuszkiewicz E., 1988, ApJ, 332, 646
Arnaud K. A., 1996, in Jacoby G. H., Barnes J., eds, ASP Conf. Ser. Vol. 101, Astronomical Data Analysis Software and Systems V. Astron. Soc. Pac., San Francisco, p. 17
Bagińska P., Różańska A., Czerny B., Janiuk A., 2021, ApJ, 912, 110
Begelman M. C., Pringle J. E., 2007, MNRAS, 375, 1070
Ciesielski A., Wielgus M., Kluźniak W., Sądowski A., Abramowicz M., Lasota J. P., Rebusco P., 2012, A&A, 538, A148
Davis S. W., Hubeny I., 2006, ApJS, 164, 530
Dexter J., Scepi N., Begelman M. C., 2021, ApJ, 919, L20
Done C., Kubota A., 2006, MNRAS, 371, 1216
Done C., Gierliński M., Kubota A., 2007, A&AR, 15, 1
EHT Collaboration, 2019, ApJ, 875, L1
Giacconi R., Kellogg E., Gorenstein P., Gursky H., Tananbaum H., 1971, ApJ, 165, L27
Gierliński M., Done C., 2004, MNRAS, 347, 885
Gladstone J. C., Roberts T. P., Done C., 2009, MNRAS, 397, 1836
Gronkiewicz D., Różańska A., 2020, A&A, 633, A35
Homan J., Wijnands R., van der Klis M., Belloni T., van Paradijs J., Klein-Wolt M., Fender R., Méndez M., 2001, ApJS, 132, 377
Kaaret P., Feng H., Roberts T. P., 2017, ARA&A, 55, 303
King A. R., 2009, MNRAS, 393, L41
King A. R., Davies M. B., Ward M. J., Fabbiano G., Elvis M., 2001, ApJ, 552, L109
Kluzniak W., Kita D., 2000, ApJ, preprint (arXiv:astro-ph/0006266)
Kubota A., Makishima K., 2004, ApJ, 601, 428
Kulkarni A. K. et al., 2011, MNRAS, 414, 1183
Lančová D. et al., 2019, ApJ, 884, L37
Lasota J.-P., 2001, New Astron. Rev., 45, 449
Lasota J. P., Vieira R. S. S., Sądowski A., Narayan R., Abramowicz M. A., 2016, A&A, 587, A13
Levine A. M., Bradt H., Cui W., Jernigan J. G., Morgan E. H., Remillard R., Shirey R. E., Smith D. A., 1996, ApJ, 469, L33
Lightman A. P., Eardley D. M., 1974, ApJ, 187, L1
Li L.-X., Zimmerman E. R., Narayan R., McClintock J. E., 2005, ApJS, 157, 335
McClintock J. E., Shafee R., Narayan R., Remillard R. A., Davis S. W., Li L.-X., 2006, ApJ, 652, 518
McClintock J. E., Narayan R., Steiner J. F., 2014, Space Sci. Rev., 183, 295
Méndez M., van der Klis M., 1997, ApJ, 479, 926
Middleton M., Done C., Gierliński M., Davis S. W., 2006, MNRAS, 373, 1004
Mishra B., Begelman M. C., Armitage P. J., Simon J. B., 2020, MNRAS, 492, 1855
Mondal S., Różańska A., Bagińska P., Markowitz A., De Marco B., 2021, A&A, 651, A54
Motta S. E., Kajava J. J. E., Sánchez-Fernández C., Giustini M., Kuulkers E., 2017, MNRAS, 468, 981
Narayan R., McClintock J. E., 2005, ApJ, 623, 1017
Narayan R., Zhu Y., Psaltis D., Sądowski A., 2016, MNRAS, 457, 608
Narayan R., Sądowski A., Soria R., 2017, MNRAS, 469, 2997
Novikov I. D., Thorne K. S., 1973, in Dewitt C., Dewitt B. S., eds, Black Holes (Les Astres Occlus). Gordon Breach, New York, NY, p. 343
Oda H., Machida M., Nakamura K. E., Matsumoto R., 2009, ApJ, 697, 16
Ogawa T., Ohsuga K., Makino Y., Mineshige S., 2021, PASJ, 73, 701
Ohsuga K., Mineshige S., 2011, ApJ, 736, 2
Ohsuga K., Mineshige S., Mori M., Kato Y., 2009, PASJ, 61, L7
Page D. N., Thorne K. S., 1974, ApJ, 191, 499
Regev O., Gitelman L., 2002, A&A, 396, 623
Remillard R. A., McClintock J. E., 2006, ARA&A, 44, 49
RóżaŃska A., Czerny B., Życki P. T., Pojmański G., 1999, MNRAS, 305, 481
Różańska A., Madej J., Konorski P., SaĎowski A., 2011, A&A, 527, A47
Różańska A., Malzac J., Belmont R., Czerny B., Petrucci P.-O., 2015, A&A, 580, A77
Shakura N. I., Sunyaev R. A., 1973, A&A, 500, 33
Shakura N. I., Sunyaev R. A., 1976, MNRAS, 175, 613
Sikora M., 1981, MNRAS, 196, 257
Steiner J. F., McClintock J. E., Remillard R. A., Narayan R., Gou L., 2009, ApJ, 701, L83
Steiner J. F., McClintock J. E., Orosz J. A., Remillard R. A., Bailyn C. D., Kolehmainen M., Straub O., 2014, ApJ, 793, L29
Straub O. et al., 2011, A&A, 533, A67
Sutton A. D., Roberts T. P., Middleton M. J., 2013, MNRAS, 435, 1758
Sądowski A., 2009, ApJS, 183, 171
Sądowski A., 2016, MNRAS, 459, 4397
Sądowski A., Narayan R., 2015, MNRAS, 454, 2372
Sądowski A., Abramowicz M., Bursa M., Kluźniak W., Lasota J. P., Różańska A., 2011, A&A, 527, A17
Sądowski A., Narayan R., Tchekhovskoy A., Zhu Y., 2013, MNRAS, 429, 3533
Sądowski A., Narayan R., McKinney J. C., Tchekhovskoy A., 2014, MNRAS, 439, 503
Sądowski A., Wielgus M., Narayan R., Abarca D., McKinney J. C., Chael A., 2017, MNRAS, 466, 705
Vincent F. H., Paumard T., Gourgoulhon E., Perrin G., 2011, Class. Quantum Gravity, 28, 225011
Wielgus M., Yan W., Lasota J. P., Abramowicz M. A., 2016, A&A, 587, A38
Zdziarski A. A., Johnson W. N., Magdziarz P., 1996, MNRAS, 283, 193
Zhang S. N., Cui W., Chen W., Yao Y., Zhang X., Sun X., Wu X.-B., Xu H., 2000, Science, 287, 1239
Zhu Y., Narayan R., 2013, MNRAS, 434, 2262
Zhu Y., Narayan R., Sądowski A., Psaltis D., 2015, MNRAS, 451, 1661
Życki P. T., Done C., Smith D. A., 1999, MNRAS, 309, 561

This paper has been typeset from a TEX/LATEX file prepared by the author.